J Solid State Electrochem (2016) 20:3263–3270
DOI 10.1007/s10008-016-3231-6

ORIGINAL PAPER

Quartz crystal microbalance electrode modified with thermoresponsive crosslinked and non-crosslinked *N*-isopropylacrylamide polymers. Response to changes in temperature

Kamil Marcisz[1] · **Marcin Karbarz**[1] · **Zbigniew Stojek**[1]

Received: 19 March 2016 / Revised: 24 April 2016 / Accepted: 26 April 2016 / Published online: 6 May 2016

Abstract Electrochemical quartz crystal microbalance (EQCM) electrode was modified with environmentally sensitive polymers. The polymer layers on the electrode were composed of either crosslinked or non-crosslinked thermoresponsive poly(*N*-isopropylacrylamide). For anchoring thin gel films on the electrode surface, the electrochemically induced free radical polymerization (EIFRP) was employed. The electroreduction of the peroxydisulfate anion led to generation of free radical. This radical initiated the free radical polymerization process that led to the formation of a thin gel layer attached to the electrode surface. To monitor in situ the growth of the polymer film the changes in resonant frequency of the quartz crystal were recorded. A significant decrease in the frequency (growth of the layer) was seen in the potential range where the reduction of peroxydisulfate anion took place. The morphology of the layers was examined with a scanning electron microscopy (SEM). The phenomenon of volume phase transition (shrinking/swelling process) in the gel layers initiated by a change in temperature was investigated. Unexpected big, sharp, and of negative sign minima appeared at the change-in-frequency vs. temperature plots. These minima were not seen in the plots obtained for the polymers without linker. That situation should be useful in the investigation of chemical interactions proceeding under the conditions of volume phase transition. The influence of volume phase transition on the transport of a member of a model red-ox system, ferro- and ferricyanide couple, and therefore on height of its voltammetric response was examined. The changes in electrochemical properties of the layers induced by volume phase transition were monitored with electrochemical impedance spectroscopy.

Keywords Thermoresponsive gels · Electrochemical quartz crystal microbalance · Crosslinked NIPA polymer · Electrochemically induced free radical polymerization

✉ Zbigniew Stojek
stojek@chem.uw.edu.pl

[1] Faculty of Chemistry, University of Warsaw, Pasteura 1, 02-093 Warsaw, Poland

Introduction

Polymer gels are defined as macromolecules that form a three-dimensional network, which is filled with solvent. The content of the solvent in many cases reaches 95 % *w/w*. These materials have properties of solids and liquids. One of the most intriguing properties of polymeric gels is their reversible volume phase transition. This phenomenon involves the transition of the gel from a swollen state to a shrunken state or vice versa. The volume of a gel can decrease even by a factor of one thousand what makes polymer gel very attractive. The reversible phase transition occurs in response to changes in the environmental conditions (e.g., in temperature, pH, ionic strength, presence of specific ions, pressure, solvent composition, and electromagnetic radiation). [1–7].

The ability of the gels to adapt to changing external conditions resulted in calling them "smart" materials. Because of their environmental sensitivity and unique structure, these polymeric hydrogels have been employed in a variety of fields, e.g., in controlled drug release systems, artificial muscles, sensors, molecular recognition systems, and as specific sorbents. Their attachment to the surface of an electrode improves their usefulness in, e.g., surface patterning, construction of switchable sensors/biosensors and more [8–16].

The intriguing types of hydrogels are thermoresponsive gels. Among them, the gels based on poly(N-

isopropylacrylamide) (pNIPA), which exhibit a drastic swelling transition at their lower critical solution temperature of ca. 33 °C, are most interesting. Below 33 °C these gels are swollen, whereas above 33 °C they dehydrate to the collapsed state; the interactions between the hydrophobic groups become stronger and water is expelled from the gel network [17–21].

So far the deposition of polymers on the surface of EQCM electrode was usually done by preliminary functionalization of the surface and then, by using appropriate reaction, the polymer was grafted [22–25]. The deposition of pNIPA gels on Au EQCM electrode using electrochemical induced polymerization was already presented; however, the electropolymerization was carried out using chronoamperometry [26]. In our previous work the electropolymerization, via cyclic voltammetry, of interpenetrating networks was done on the platinum surface. The polymerization process was monitored using a quartz crystal microbalance. However, in that paper, frequency change at the EQCM electrode was not examined under the conditions of the volume phase transition [27]. There are a few literature reports on EQCM response to layers of pNIPA [26, 28, 29]. These reports are somewhat contradictive; the presented EQCM responses differed much regarding the appearance of sharp, unexpected minima in the recorded output. This fact triggered our investigation. We have made an effort to find conditions of monitoring the frequency changes not loaded with the unwanted phenomena.

In this paper, the electrochemically induced free radical polymerization method was used to anchor gels on gold electrode surface via cyclic voltammetry. There was no need for any preliminary functionalization of the surface. The electrode was placed in a solution containing the monomers and sodium peroxydisulfate. After imposing a sufficiently negative potential, the electroreduction of the peroxydisulfate anion started and the radical was formed. This radical initiated the free radical polymerization process that led to the formation of a thin gel layer attached to the gold electrode surface.

The modified Au EQCM electrodes were examined under the conditions of volume phase transition in the deposited layers. Thin pNIPA layers with and without crosslinker were employed. In characterization of the layers, cyclic voltammetry and electrochemical impedance spectroscopy (EIS) measurements with the ferro- and ferricyanide anions were performed.

Experimental

Materials

N-Isopropylacrylamide (NIPA, 97 %), *N*,*N*′-methylenebisacrylamide (BIS, 99 %), ammonium peroxydisulfate (APS, 99.99 %), and sodium nitrate ($NaNO_3$, 99 %) were purchased from Aldrich. The electroactive probes, potassium ferro- and ferricyanide (98 %), were also purchased from Aldrich. All chemicals were used as received except for NIPA, which was recrystallized from a toluene/hexane mixture (30:70 *v*/*v*). All solutions were prepared using high purity water obtained from a Milli-Q Plus/Millipore purification system (conductivity of water: 0.056 $mScm^{-1}$).

Electrochemical measurements

All electrochemical measurements were performed using a CH-Instruments model CHI 400B potentiostat controlled via manufacturer's software. The three-electrode system was used. A platinum wire and a saturated silver chloride (Ag/AgCl/sat. KCl) electrode were used as the counter and the reference electrode, respectively. A Au EQCM was used as the working electrode. The electrodes were kept in a water-jacketed glass cell. Temperature of that cell was controlled using a refrigerated circulator (Polystat, Cole-Parmer). To minimize the electric noise, the electrochemical cell was kept in a grounded, covered with aluminum-foil Faraday cage.

The electrochemical impedance spectroscopy (EIS) measurements were performed using a CH-Instruments model CHI 750D potentiostat, in solution of ferro-ferricyanide couple, at its formal potential, in the frequency range from 100 kHz to 0.1 Hz. An alternating voltage of 10 mV was used. The data were processed using an EIS Spectrum Analyzer. The equivalent electronic circuit selected for the fitting process included the electrolyte resistance (R_s), Warburg impedance (Z_w), electron transfer resistance (R_{et}), and the constant phase element Q (instead of the double layer capacitance, C_{dl}).

EQCM measurements

An electrochemical quartz crystal microbalance module for CHI-Instruments, model CHI 400B potentiostat with 8-MHz Au/TiO_2 quartz crystal resonator was used. The EQCM technique allowed to record simultaneously voltammetric/chronoamperometric and microgravimetric curves. The resonant frequency of the quartz crystal lattice was measured in function of the mass attached to the crystal interface. For a thin rigid film, the interfacial mass change, Δm, is related to the shift in resonance oscillation frequency, Δf, of the EQCM through the Sauerbrey equation:

$$\Delta \mathrm{f} = -\frac{2f_0^2}{A\sqrt{\rho_q \mu_q}}\Delta \mathrm{m} \quad (1)$$

where f_0 is the oscillation frequency in the fundamental mode, A is the piezoelectrically active surface area, ρ_q is the density of quartz (ρ_q = 2.648 gcm^{-3}), and μ_q is the shear modulus of

quartz ($\mu_q = 2.947 \times 10^{11}$ gcm^{-1} s^{-2}). All experimental variables influencing the resonant frequency of the EQCM electrodes such as pressure, viscosity, and density of the solution were kept constant during the measurements [30].

In our case, we should use the above form of Sauerbrey's equation with caution. The equation is correct for thin homogenous rigid films. Thin films based on crosslinked and non-crosslinked pNIPA exhibit properties of thin laterally homogenous viscoelastic films, where dissipation of energy takes place due to viscoelastic properties of the polymer. In this work, EQCM technique was used only for qualitative monitoring of the volume phase transition phenomena. For quantitative calculations the Sauerbrey equation should be appropriately modified [31].

SEM measurements

A scanning electron microscope (SEM, Zeiss Merlin field emission) equipped with an energy dispersive spectrometer (Bruker, EDS) was used for the examination of the modified electrode surfaces.

Modification of EQCM electrodes with pNIPA gel

Before the polymerization process, the EQCM Au/TiO_2 electrodes were treated with hot piranha solution to remove organic pollutants, rinsed with water, and then dried with ethanol. Then, the electrodes were placed in a special home-made Teflon case (see Fig. 1). Next, the electrodes were immersed in a degassed aqueous solution containing NIPA monomer (0.693 M), crosslinker monomer (7 mM, BIS), and an initiator of the polymerization (10 mM, APS). Additionally, the solution contained $NaNO_3$ (0.2 M) as the supporting electrolyte. The radicals needed for starting the polymerization were formed continuously by doing 60 cyclic polarizations of the Au electrode between −0.1 and −1.1 V vs. the Ag/AgCl electrode at a rate of 100 mVs^{-1}. To monitor in situ the growth of the polymer film, we used an electrochemical quartz crystal microbalance. The electrode modified with gel was immersed into deionized water for 1 day to wash away the residual chemicals. During the washing time, water was exchanged several times.

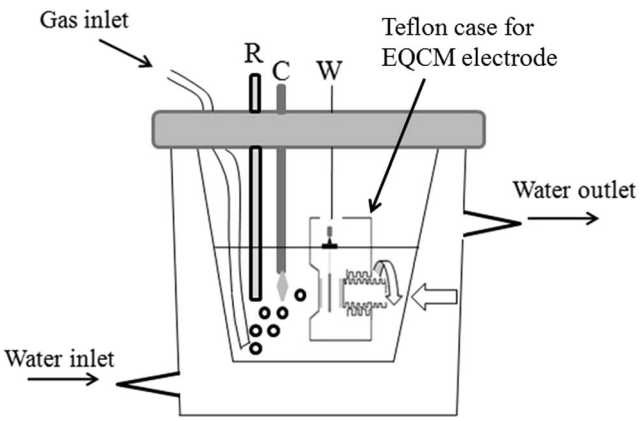

Fig. 1 Scheme of electrochemical measurement system. Silver chloride reference electrode (*R*), working gold EQCM electrode (*W*), and Pt wire as counter electrode (*C*)

Results and discussion

In Fig. 2a, representative voltammograms obtained with a EQCM electrode in a solution containing NIPA monomer (without linker) and supporting electrolyte before (dashed line) and after addition of APS (solid line) are presented. Typical frequency shifts obtained in the solution during the voltammetric cycling are presented in Fig. 2b. Figure 3a and b

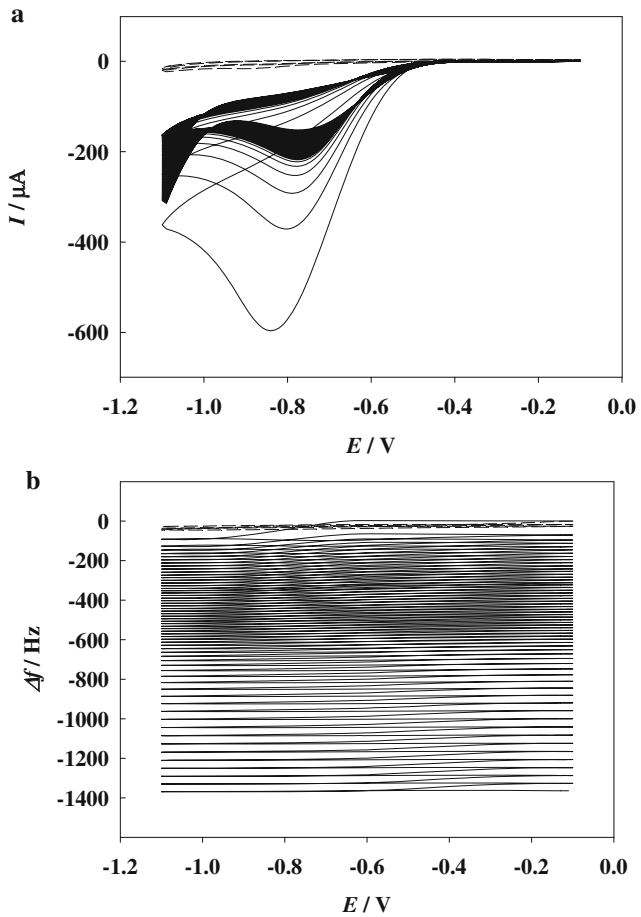

Fig. 2 **a** Consecutive voltammograms obtained during modification of electrode surface in deoxygenated solution containing either NIPA monomer with initiator (*solid line*) or without initiator (*dashed line*). **b** Frequency shift, Δf, during modification of electrode surface in deoxygenated solution containing either NIPA monomer with initiator (*solid line*) or without initiator (*dashed line*)

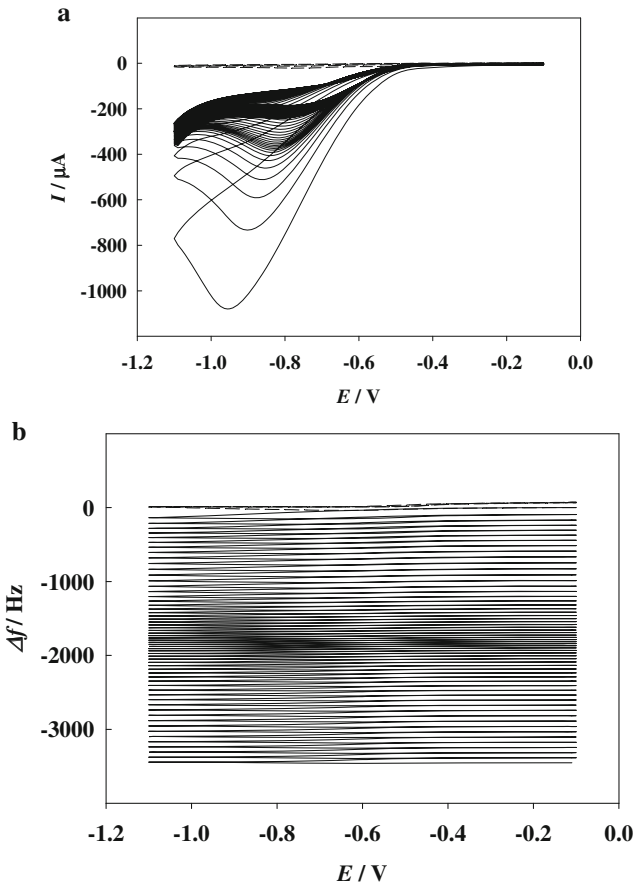

Fig. 3 **a** Successive voltammograms obtained during modification of electrode surface in deoxygenated solution containing either NIPA monomer with initiator (*solid line*) or without initiator (*dashed line*). **b** Frequency shift, Δf, during modification of electrode surface in deoxygenated solution containing either NIPA monomer with initiator (*solid line*) or without initiator (*dashed line*)

presents voltammograms and frequency shifts during the process of polymerization in solution containing NIPA monomer, BIS crosslinker, and supporting electrolyte before (dashed line) and after addition of APS (solid line), respectively. No current peak was observed at dashed line voltammograms in Figs. 2a and 3a. Simply in the absence of APS no faradaic current was seen. After addition of the initiator, APS voltammetric peaks appeared and the polymerization reaction started, see frequency changes in Figs. 2b and 3b. According to Sauerbrey's Eq. (1), these frequency shifts in the quartz crystal corresponded to the changes in polymer mass on the crystal surface. The decrease in the resonant oscillation frequency in the quartz crystal was well correlated with the cyclic electroreduction of the peroxydisulfate ions. Interestingly, for a polymer layer without the crosslinker, the decrease in frequency was much slower. After 60 voltammetric cycles, the total shift of frequency was circa 1400 Hz (see Fig. 2b), while for the polymer layer containing the BIS crosslinker the total shift of frequency reached 3500 Hz (see Fig. 3b). It seems that the bigger change in the quartz frequency in the case of the crosslinked polymer can reflect a bigger amount of attached polymer to the surface and the more extensive hydration of the polymer nets due to bigger spaces between the polymer strands.

N-Isopropylacrylamide is a thermoresponsive polymer exhibiting a volume phase transition at 33 °C. That volume phase transition was examined on the EQCM electrode surface. For this purpose the electrode was placed in water in a thermostated vessel. Temperature was changed from 20 to 45 °C.

Typical frequency shift obtained for a EQCM electrode covered with a layer of non-crosslinked pNIPA polymer is plotted as a function of temperature/time in Fig. 4a. In the case of uncovered electrode, an increase in temperature leads to a small increase in frequency of quartz crystal by circa 300 Hz. However, in the case of an electrode modified with pNIPA polymer, the volume phase transition (taking place at 33 °C) led to a quick, substantial frequency increase to value circa 1000 Hz and stayed at this level. This increase corresponds to a loss of weight on the electrode surface. Next, the solution was cooled to 20 °C. Already, the temperature decrease to 32 °C caused the regaining of the initial frequency value. Simply the polymer chains became hydrated and swelled again and the mass on the electrode surface increased. Temperature of the volume phase transition appeared to be different in the heating and the cooling processes. Similar effect was observed in the investigation of the pNIPA volume phase transition by, e.g., differential scanning calorimetry [32]. It is presumably due to the formation of intra- and interchain hydrogen bonds in the collapsed state.

Characteristic frequency shift obtained for a EQCM electrode covered with crosslinked pNIPA gel in function of time is presented in Fig. 4b. A distinct difference between non-crosslinked and crosslinked layers of pNIPA can be seen. Firstly, unexpected decreases in frequency to very negative values, both before the shrinking process and before the swelling process, were observed in the case of crosslinked pNIPA gel. The frequency minimum reached the values much lower than the initial frequency. In the case of the shrinking process,

Fig. 4 **a** Frequency shift of quartz crystal plotted as function of time (for relation between time and temperature see *dotted line* in the *bottom*). Electrode modified with non-crosslinked pNIPA—*solid line*, unmodified EQCM electrode—*dashed line*. *Inset*: frequency shift as function of temperature for electrode modified with non-crosslinked pNIPA (*solid line*) and unmodified EQCM electrode (*dashed line*). **b** Frequency shift for electrode modified with pNIPA crosslinked with BIS (*solid line*) and unmodified EQCM electrode (*dashed line*). *Inset*: frequency shift as function of temperature for electrode modified with pNIPA crosslinked with BIS (*solid line*) and unmodified EQCM electrode (*dashed line*)

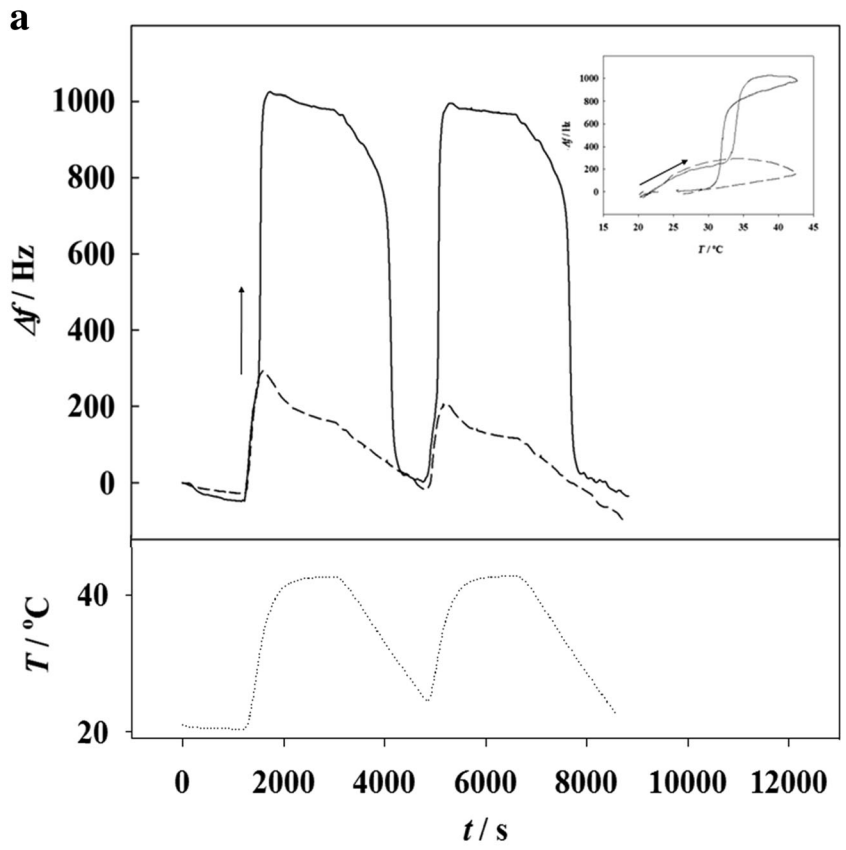
a
Δf / Hz
T / °C
t / s
0
2000
4000
6000
8000
10000
12000
20
40
200
400
600
800
1000

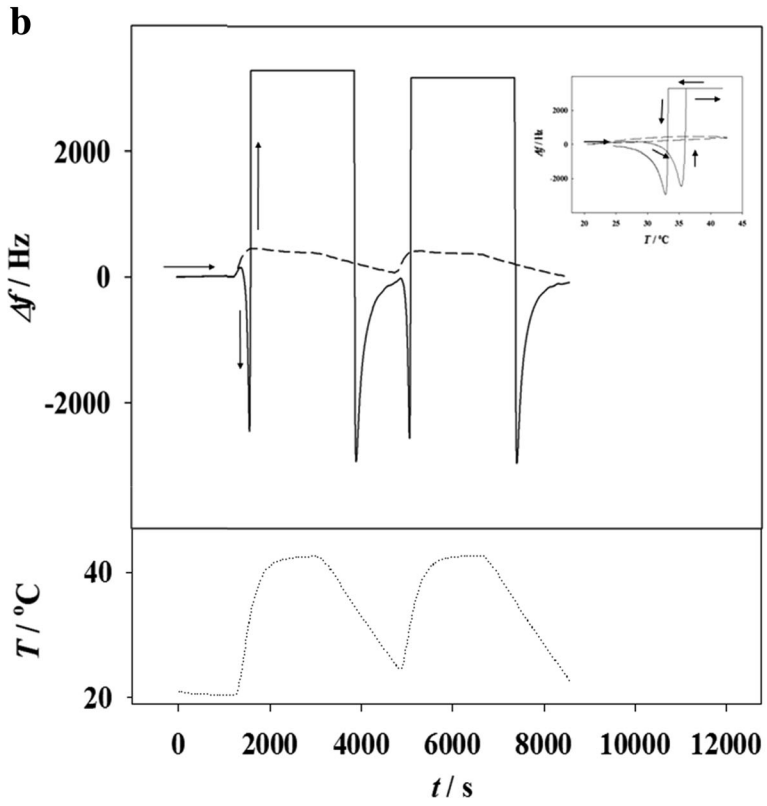
b
Δf / Hz
T / °C
t / s
0
2000
4000
6000
8000
10000
12000
20
40
-2000
0
2000

it might be caused by formation of tighter net on the surface of the gel layer in the first stage of the process. As a result, the electrode could feel a bigger load. Regarding the swelling process, it might be possible that initially the net absorbs an excessive amount of water and finally reaches the equilibrium. The differences in the behavior of both materials (crosslinked and non-crosslinked) can also reflect the difference in the process of changing the volume of thin gel layers. The non-crosslinked layer of pNIPA hydrogel attached to the gold surface can shrink and swell only in the direction perpendicular to the surface. Whereas the crosslinked network has a tendency to shrink and swell in all directions and can therefore generate extra forces in the system. Finally, the unexpected frequency minima may reflect the mechanical, vibrating reaction of the 3D net to strong streams of water in and out of the net.

The final values of frequency obtained after the shrinking process and after the swelling process are in agreement with our expectations and clearly depict the loss and gain of water by the crosslinked and non-crosslinked polymers. Apparently, the amount of water absorbed by the crosslinked polymer is much bigger compared to non-crosslinked polymer. In the case of crosslinked polymer, the increase in frequency exceeds the allowable instrumental output and therefore a plateau is seen in the plot. The effect presented in Fig. 4 is really very interesting and indicates that the volume phase transition from the swollen to the shrunken state and vice versa is not a straightforward phenomenon. This unexpected behavior of crosslinked pNIPA layer was well repeatable in the experiments. However, in the literature, for a crosslinked pNIPA layer obtained via chronoamperometric electropolymerization, that behavior was not observed [26]. The minima were shown in two other papers [28, 29]. They were explained in terms of changing the polymer structure and coupling of the layer to the surrounding fluid. Apparently, the anomalies visible in the Δf plots are not helpful in the use of EQCM in the investigation of interactions between the molecules/drugs and the anchored biomacromolecules under the conditions of volume phase transition. Fortunately, we have found that the volume phase transition in non-crosslinked pNIPA is not accompanied by the above unwanted Δf minima.

The changes in properties of non-crosslinked and crosslinked pNIPA layers caused by changes in temperature (involving the volume phase transition) were examined with the use of an electroactive probe (ferro- and ferricyanide system). Two techniques were employed: CV and EIS. The electroeduction and electrooxidation of ferro- and ferricyanide ions at a gold electrode is a reversible one-electron reaction. The electrochemical measurements were performed in a temperature range 20–45 °C, which includes the volume phase transition of the gel layers. In Fig. 5a and b, typical cyclic voltammetric curves for non-crosslinked- and crosslinked pNIPA layers are presented, respectively. In both cases, the

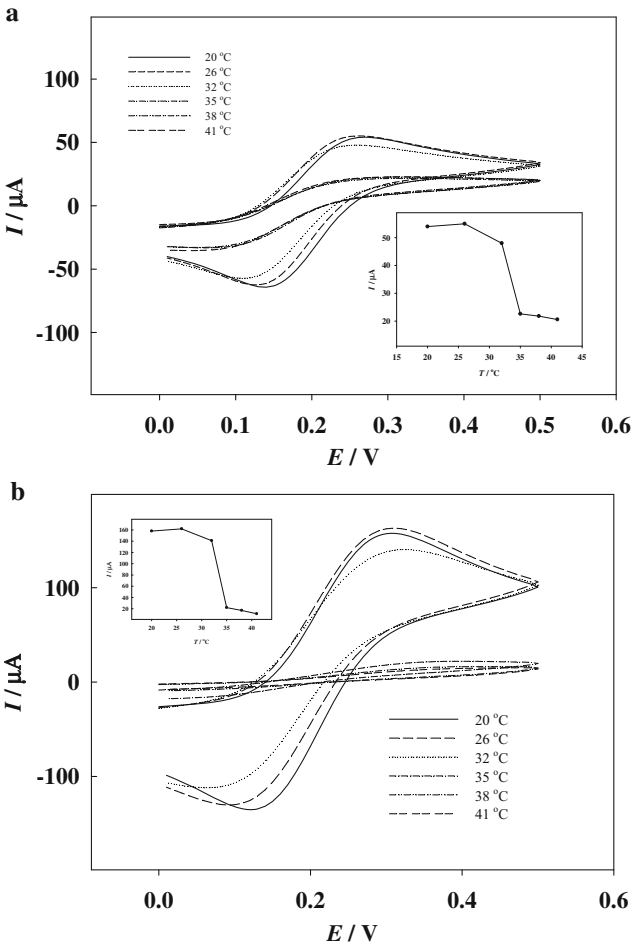

Fig. 5 Voltammograms obtained for oxidation and reduction of ferro- and ferricyanide system at EQCM electrode modified with pNIPA (**a**) and pNIPA BIS (**b**) at different temperatures. *Inset*: peak current of oxidation of $Fe(CN)_6^{4-}$ at modified EQCM electrode in function of temperature

reduction and oxidation peaks presented lower current values after the volume phase transition (at temperature higher than 33 °C); the drop was particularly substantial in the second case. It was so because in the swollen state the polymer chains were separated, and diffusion of electroactive species was not extensively limited. Contrary, after the volume phase transition, when the polymer is in the shrunken state, the penetration of the polymer layer by the electroactive species is more difficult, so the reduction and oxidation peaks presented lower current values.

Next technique used to characterize the layer properties was electrochemical impedance spectroscopy (EIS). Figure 6a and b presents typical Nyquist plots for modified electrodes at different temperatures. The semicircle diameter corresponds to electron transfer resistance of the ferro-/ferricyanide process. At 20 °C, in both cases, electron transfer resistance was low. For non-crosslinked pNIPA layers, the

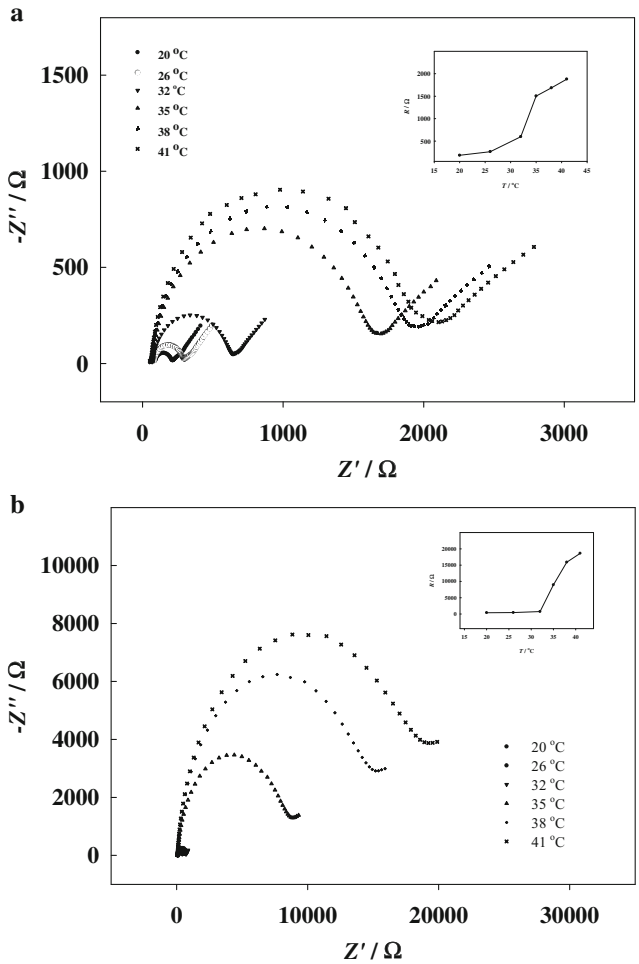

Fig 6 Impedance spectra obtained at different temperatures for pNIPA (**a**) and pNIPA BIS (**b**) films. *Insets*: changes in electron transfer resistance in function of temperature for thin polymer films

increase in temperature affected the resistance value. The highest increase in resistance took place after reaching the temperature of VPT. For crosslinked pNIPA layers, the situation was similar; however, the maximum electron transfer resistance reached a much higher value of circa 19,000 Ω, compared to circa 2000 Ω.

To characterize the morphology of the surface of the modified electrodes, a scanning electron microscope was used. The gel layers were analyzed in their dry state. Figure 7a and b presents photos of the electrodes modified with non-crosslinked and crosslinked pNIPA layers, respectively. In both cases, the polymer formed planar, thin, and homogenous layers. The electrode surface was partially uncovered to show the differences between the bare electrode surface and the polymer layer. The detached layer was apparently uniform and its thickness was estimated to be circa 200 nm for non-crosslinked and 500 nm for crosslinked pNIPA layer.

Conclusions

A quartz crystal microbalance was used to monitor in situ the electrodeposition of non-crosslinked and crosslinked pNIPA polymers on the surface of a gold electrode. Electrochemically induced free radical polymerization was used for synthesis of the polymer layers. The layers were thin, very stable in time, and thermoresponsive. The productivity of electrodeposition of crosslinked polymer was much bigger compared to non-crosslinked polymer.

To monitor the volume phase transition caused by a change in temperature, the EQCM technique was used. It can be seen that non-crosslinked and crosslinked pNIPA layers behaved very differently. An unexpected change in the quartz frequency related to the volume phase transition was observed for crosslinked pNIPA layers; before both shrinking and swelling processes, the frequency of the quartz dropped to very negative values. The literature reports on EQCM response on the phase transition are somewhat confusing. On some curves there is no minima, on others the minima are not so spectacular [26, 28, 29]. In our investigations, the differences in the

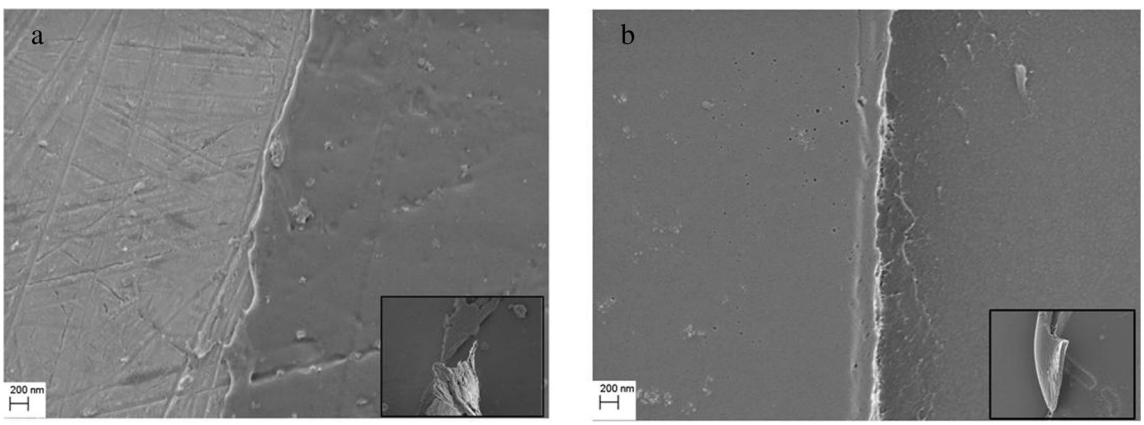

Fig. 7 SEM images of EQCM electrode surface covered by pNIPA (**a**) and pNIPA BIS polymer (**b**) and partially uncovered by scratching. *Insets*: Magnified parts of detached layers

behavior of both materials (crosslinked and non-crosslinked) can be related to the difference in the process of changing the volume of thin gel layers attached to the electrode surface. In a crosslinked layer of pNIPA, the effect of shrinking and swelling is also present in the parallel direction to the electrode surface and can therefore generate extra forces in the system. In addition, the unexpected frequency minima may reflect the mechanical, vibrating reaction of the 3D net to strong streams of water in and out of the net. Apparently, the anomalies visible in the Δf plots (obtained for crosslinked gels) disable a possibility of using EQCM in the investigation of interactions between various molecules and biomacromolecules attached to the electrode surface under the conditions of volume phase transition. This possibility remains for non-crosslinked pNIPA, where the volume phase transition is not accompanied by the unwanted Δf minima.

To examine the consequences of volume phase transition to electrode processes, cyclic voltammetry and electrochemical impedance spectroscopy measurements were done. The differences in the height of the oxidation/reduction peaks of the red-ox probe, before and after the shrinking process and between the non-crosslinked and crosslinked polymers, were substantial. Correspondingly, the EIS measurements demonstrated that the charge transfer resistance increased substantially after the shrinking process. The volume phase transition in the polymer layers was well reversible and the layers were stable for at least 1 month.

Acknowledgements This work was supported by a Iuventus grant no. IP2011 022471 from the Ministry of Science and Higher Education of Poland and and by a grant no. 2011/01/D/ST5/05866 from the National Science Center of Poland.

References

1. Deng J, Qinxiong H, Zhilin W, Yang W (2008) J Polym Sci Part A Polym Chem 46:2193–2201
2. Li P, Kim NH, Siddaramaiah H, Lee JH (2009) Compos Part B 40: 275–283
3. Pafiti KS, Philippou Z, Loizou E, Porcar L, Patrickios CS (2011) Macromolecules 44:5352–5362
4. Ju XJ, Chu LY, Liu L, Mi P, Lee YM (2008) J Phys Chem B 112: 1112–1118
5. Itahara T, Tsuchida T, Morimoto M (2010) Polym Chem 1:1062–1066
6. Wang L, Liu M, Gao C, Ma L, Cui D (2010) React Funct Polym 70: 159–167
7. Zhou L, He B, Zhang F (2012) ACS Appl Mater Interfaces 4:192–199
8. Tao Y, Ai L, Bai H, Liu X (2012) J Polym Sci Part A Polym Chem 17:3507–3516
9. Mahkam M, Biomed J (2005) Mater Res Part B 75:108–112
10. Hyk W, Karbarz M, Stojek Z, Ciszkowska M (2004) J Phys Chem B 108:864–868
11. Karbarz M, Romanski J, Michniewicz K, Jurczak J, Stojek Z (2010) Soft Matter 6:1336–1342
12. Tokuyama H (2007) IwamaT. Langmuir 23:13104–13108
13. Romanski J, Karbarz M, Pyrzynska K, Jurczak J, Stojek Z (2012) J Polym Sci Part A: Polym Chem 50:542–550
14. Liang Y, Song S, Yao H, Hu N (2011) Electrochim Acta 56:5166–5173
15. Tam TK, Pita M, Motornov M, Tokarev I, Minko S, Katz E (2010) Electroanalysis 22:35–40
16. Klis M, Karbarz M, Stojek Z, Rogalski J, Bilewicz R (2009) J Phys Chem 113:6062–6067
17. Kristesen TE, Hansen T (2010) Eur J Org Chem 17:3179–3204
18. Karbarz M, Pyrzynska K, Romanski J, Jurczak J, Stojek Z (2010) Polymer 51:2959–2964
19. Bignotti F, Penco M, Sartore L, Peroni I, Mendichi R, Casolaro M, D'Amore A (2000) Polymer 41:8247–8256
20. Casolaro M, Battari S, Ito Y (2006) Biomacromolecules 7:1439–1448
21. Karbarz M, Pulka K, Misicka A, Stojek Z (2006) Langmuir 22: 7843–7847
22. Annaka M, Yahiro C, Nagase K, Kikuchi A, Okano T (2007) Polymer 48:5713–5720
23. Liu GM, Zhang GZ (2005) J Phys Chem B 109:743–747
24. Zhang GZ (2004) Macromolecules 37:6553–6557
25. Piacham T, Josell A, Arwin H, Prachayasittikul V, Ye L (2005) Anal Chim Acta 536:191–196
26. Reuber J, Reinhardt H, Johannsmann D (2006) Langmuir 22:3362–3367
27. Kaniewska K, Karbarz M, Stojek Z (2015) Electrochim Acta 179: 372–378
28. Ishida N, Biggs S (2007) Langmuir 23:11083–11088
29. Heinz P, Bretagnol F, Mannelli I, Sirghi L, Valsesia A, Ceccone G, Gilliland D, Landfester K, Rauscher H, Rossi F (2008) Langmuir 24:6166–6175
30. Sauerbrey G (1959) Z Phys 155:206–222
31. Reviakine I, Johannsmann D, Richter RP (2011) Anal Chem 83: 8838–8848
32. Gao Y, Yang J, Ding Y, Ye X (2014) J Phys Chem B 118:9460–9466